

## Effects of surface tension and viscosity on the growth rates of Rayleigh-Taylor and Richtmyer-Meshkov instabilities

Sung-Ik Sohn\*

*Department of Mathematics, Kangnung-Wonju National University, Kangnung 210-702, South Korea*  
(Received 25 May 2009; revised manuscript received 6 November 2009; published 24 November 2009)

We present an analytical model for unstable interfaces with surface tension in fluids of arbitrary viscosity. Linear and nonlinear asymptotic solutions are obtained for growth rates of Rayleigh-Taylor and Richtmyer-Meshkov instabilities. In Rayleigh-Taylor instability, both surface tension and viscosity decrease the asymptotic bubble velocity. For Richtmyer-Meshkov instability, the analysis of the model suggests a dependence of the decaying rate of the bubble velocity on the relative importance of viscosity and surface tension. Results of numerical simulations are also given, and comparisons of the solutions of the model with numerical results are in good agreement.

DOI: [10.1103/PhysRevE.80.055302](https://doi.org/10.1103/PhysRevE.80.055302)

PACS number(s): 47.20.Ma, 47.20.Ky

Unstable fluid mixing occurs frequently in basic science and engineering applications. A gravity-driven interfacial instability is known as Rayleigh-Taylor (RT) instability [1] and a shock-driven interfacial instability is known as Richtmyer-Meshkov (RM) instability [2]. The RT and RM instabilities play important roles in many fields ranging from astrophysics to inertial confinement fusion. Since Rayleigh [1] and Richtmyer [2] first considered these problems, they have received attentions in a wide range of contexts, but many aspects of dynamics of the instabilities are still uncertain.

Small perturbations at these unstable interfaces grow into nonlinear structures in the form of bubbles and spikes [3]. At a late time, a bubble in RT instability attains a constant velocity, while a RM bubble has a decaying growth rate. Eventually, turbulent mixing caused by vortex structures around spikes breaks the ordered fluid motion.

The main purpose of this Rapid Communication is present an analytical model for the unstable interfaces with surface tension in fluids of arbitrary viscosity and find linear and nonlinear growth rates of RT and RM instabilities for all physical parameters. At linear and early nonlinear stages, surface tension and viscosity effects on RT instability are well known [4,5]: surface tension produces a cut-off wave number and viscosity decreases the growth rate at low wave number and causes damping of oscillatory solutions of high wave number. However, late time nonlinear dynamics of RT instability by surface tension and viscosity still remain undiscovered. In the case of RM instability, little is known for effects of these physical variables. We will show that dynamics of unstable interfaces are significantly influenced by surface tension and viscosity and growth rates at a late time have different behaviors, depending on surface tension and viscosity.

A theoretical model for comprehensive descriptions of the motion of unstable interfaces is the potential flow model proposed by Layzer [6]. The Layzer-type model was recently extended to the system of finite density ratios using various forms of potentials [7–11]. In this Rapid Communication, we generalize the Layzer model to the interface with surface tension and viscosity and present solutions for bubbles of RT and RM instabilities from the model.

We consider an interface, in a vertical channel of width  $D$ , between two incompressible fluids in two dimensions. The upper fluid is heavier than the lower fluid, i.e.,  $\rho_h > \rho_l$ . In this Rapid Communication, only a single-mode interface in the channel is considered, and nonlinear mode coupling and bubble merger, which occurs in the evolution of initial multimode perturbation, are not taken into account. The kinematic condition and the Bernoulli equation on the interface  $y = \eta(x, t)$  are

$$\frac{\partial \eta}{\partial t} + u_i \frac{\partial \eta}{\partial x} = v_i, \quad i = h, l, \quad (1)$$

$$[\rho(\frac{\partial \phi}{\partial t} + \frac{1}{2}|\nabla \phi|^2 + g\eta) + p] = 0, \quad (2)$$

where  $[Q] = Q_l - Q_h$ ,  $u_i$  and  $v_i$  are the  $x$  and  $y$  components of the interface velocity taken from the heavy and light fluids, and  $g$  is an external acceleration. The kinematic condition implies the continuity of the normal component of fluid velocity across the interface.

The normal stress balance on the interface is given by

$$[p] = 2[\mu \frac{\partial v}{\partial y}] - \sigma \frac{\eta_{xx}}{(1 + \eta_x^2)^{3/2}}, \quad (3)$$

where  $\mu$  is the viscosity of fluids and  $\sigma$  the surface tension of the interface. The Bernoulli equation (2) and the normal stress balance [Eq. (3)] give the dynamic equation for the interface

$$-[\rho(\frac{\partial \phi}{\partial t} + \frac{1}{2}|\nabla \phi|^2 + g\eta)] = 2[\mu \frac{\partial v}{\partial y}] - \sigma \frac{\eta_{xx}}{(1 + \eta_x^2)^{3/2}}. \quad (4)$$

The kinematic condition (1) and Eq. (4) determine the evolution of the interface.

We take the velocity potentials in Goncharov [7]

$$\phi_h = a_1(t) \cos(kx) e^{-ky}, \quad (5)$$

$$\phi_l = b_1(t) \cos(kx) e^{ky} + b_2(t)y, \quad (6)$$

where  $k = 2\pi/D$  is the wave number. The interface near the bubble tip is approximated as  $\eta = \eta_0(t) + \eta_2(t)x^2$ . Substituting this expression and the potentials into Eqs. (1) and (4) and expanding up to second order in  $x$ , we have

$$\dot{\eta}_2 = -k(3\eta_2 + \frac{k}{2})\dot{\eta}_0, \quad (7)$$

\*sohnsi@kangnung.ac.kr

$$\alpha_1 \ddot{\eta}_0 + \alpha_2 \dot{\eta}_0^2 + \alpha_3 \dot{\eta}_0 = -Ag\eta_2 + 6(1+A)\frac{\sigma}{\rho_h}\eta_2^3, \quad (8)$$

where

$$\alpha_1 = \frac{k^2 - 4Ak\eta_2 - 12A\eta_2^2}{2(k-6\eta_2)},$$

$$\alpha_2 = k^2 \frac{(4A-3)k^2 + 6(3A-5)k\eta_2 + 36A\eta_2^2}{2(k-6\eta_2)^2},$$

$$\alpha_3 = \frac{(1+A)k^2}{2\rho_h} \left[ \mu_h(k+2\eta_2) + \mu_l \frac{(k+6\eta_2)(k-2\eta_2)}{k-6\eta_2} \right],$$

and  $A = (\rho_h - \rho_l) / (\rho_h + \rho_l)$  is the Atwood number.

We first examine the linear solutions of the model. The zero-order equation of Eq. (4), after a linearization with respect to the perturbation amplitude of the interface, becomes

$$\ddot{\eta}_0 + 2\bar{\nu}k^2\dot{\eta}_0 - (Agk - \frac{\sigma}{\rho_h+\rho_l}k^3)\eta_0 = 0, \quad (9)$$

where  $\bar{\nu} = (\mu_h + \mu_l) / (\rho_h + \rho_l)$  is an average kinematic viscosity of fluids. For the RT instability ( $g = \text{const}$ ), Eq. (9) gives an exponential growth of the interface,  $\eta \sim \eta_0^0 e^{\gamma t}$  with

$$\gamma = -\bar{\nu}k^2 + \sqrt{Agk + \bar{\nu}^2k^4 - \frac{\sigma}{\rho_h+\rho_l}k^3}. \quad (10)$$

The growth rate [Eq. (10)] agrees with the result of the linear theory in Bellman and Pennington [4].

The linear solution of RM instability can be obtained by treating  $g$  as an impulsive acceleration [2], i.e.,  $g \rightarrow \delta(t)\Delta v$ , where  $\Delta v$  is the jump velocity imparted by a shock. Integrating Eq. (9) from 0- to 0+, it gives a linear growth rate of RM instability

$$\dot{\eta}_0(t) = Ak\Delta v \eta_0(0+) + 2\bar{\nu}k^2[\eta_0(0-) - \eta_0(0+)], \quad (11)$$

where  $\eta_0(0-)$  and  $\eta_0(0+)$  are the preshocked and postshocked amplitudes of the interface, respectively. We see from Eq. (11) that surface tension has no effect on the linear growth rate.

We find the asymptotic solution of a bubble in RT instability. Equation (7) can be integrated analytically, and it gives the solution for  $\eta_2$  in terms of  $\eta_0$ .

$$\eta_2(t) = \left[ \eta_2(0) + \frac{k}{6} \right] e^{-3k[\eta_0(t) - \eta_0(0)]} - \frac{k}{6}. \quad (12)$$

One may assume  $\eta_0 \rightarrow \infty$  as  $t \rightarrow \infty$  because a RT bubble keep growing by buoyancy. Then we have

$$\eta_2 \rightarrow -\frac{k}{6}. \quad (13)$$

From Eqs. (8) and (13), we obtain the bubble velocity

$$U_{RT}^{2D} \rightarrow -\frac{2}{3}k\nu_h + \sqrt{\frac{2A}{3(1+A)}\frac{g}{k} - \frac{k}{9}\frac{\sigma}{\rho_h} + \frac{4}{9}k^2\nu_h^2}, \quad (14)$$

where  $\nu_h = \mu_h / \rho_h$  is the kinematic viscosity of the heavy fluid. It is found from Eq. (14) that both surface tension and viscosity retard the asymptotic bubble velocity. The bubble velocity is also independent to the viscosity of the light fluid.

The bubble velocity [Eq. (14)] can be expressed in non-dimensional form

$$\text{Fr} = -\frac{4\pi}{3}\frac{1}{\text{Re}} + \sqrt{\frac{1}{6\pi}\frac{2A}{1+A} - \frac{2\pi}{9}\frac{1}{\text{Bo}} + \left(\frac{4\pi}{3}\frac{1}{\text{Re}}\right)^2}, \quad (15)$$

defining the Froude number  $\text{Fr} = U / \sqrt{gD}$ , the gravity Reynolds number  $\text{Re} = \sqrt{gD^3} / \nu_h$ , and the Bond number  $\text{Bo} = \rho_h g D^2 / \sigma$ .

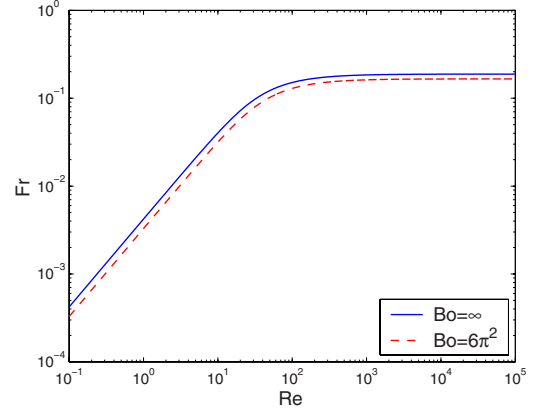


FIG. 1. (Color online) Bubble Froude number  $\text{Fr}$  vs  $\text{Re}$  for Bond numbers  $\text{Bo} = \infty$  and  $6\pi^2$ . The Atwood number is  $A = 0.5$ .

The linear growth rate [Eq. (10)] gives a stability condition for the interface. The interface should be unstable if surface tension is larger than a critical threshold,  $\sigma \geq \sigma_c = (\rho_h - \rho_l)g / k^2$ . For this critical surface tension, the bubble velocity becomes

$$U_c^{2D} = -\frac{2}{3}k\nu_h + \sqrt{\frac{4A}{9(1+A)}\frac{g}{k} + \frac{4}{9}k^2\nu_h^2}. \quad (16)$$

This equation shows that for the case of inviscid fluids, the asymptotic bubble velocity is reduced by 18% by surface tension once the interface is unstable.

Figure 1 is the bubble Froude number  $\text{Fr}$  versus  $\text{Re}$ , for Bond numbers  $\text{Bo} = \infty$  and  $6\pi^2$ , in the logarithmic scale. The Atwood number is  $A = 0.5$ . The Bond number  $\text{Bo} = 6\pi^2$  is the critical value for instability for  $A = 0.5$ . Figure 1 shows that the bubble velocity increases linearly with  $\text{Re} \lesssim 10$  and saturates at  $\text{Re} \sim 100$ . We find that the asymptotic bubble velocity is decreased greatly by viscosity.

We next consider the evolution of an axisymmetric interface in the cylindrical geometry. We take the potentials  $\phi_h = a_1(t)J_0(kr)e^{-kz}$  and  $\phi_l = b_1(t)J_0(kr)e^{kz} + b_2(t)$ , where  $J_0(x)$  is the Bessel function of zero order. After the same procedure as the two-dimensional (2D) case, we have the equations

$$\dot{\eta}_2 = -k\left(2\eta_2 + \frac{k}{4}\right)\dot{\eta}_0, \quad (17)$$

$$\alpha_1 \ddot{\eta}_0 + \alpha_2 \dot{\eta}_0^2 + \alpha_3 \dot{\eta}_0 = -Ag\eta_2 + 6(1+A)\frac{\sigma}{\rho_h}\eta_2^3, \quad (18)$$

where

$$\alpha_1 = \frac{k^2 - 4Ak\eta_2 - 32A\eta_2^2}{4(k-8\eta_2)},$$

$$\alpha_2 = k^2 \frac{(5A-4)k^2 + 16(2A-3)k\eta_2 + 64A\eta_2^2}{8(k-8\eta_2)^2},$$

$$\alpha_3 = \frac{(1+A)k^2}{4\rho_h} \left[ \mu_h(k+4\eta_2) - \mu_l \frac{(k+8\eta_2)(k-4\eta_2)}{k-8\eta_2} \right].$$

The asymptotic solution of a RT bubble in the cylindrical geometry is

$$\eta_2 \rightarrow -k/8, \quad (19)$$

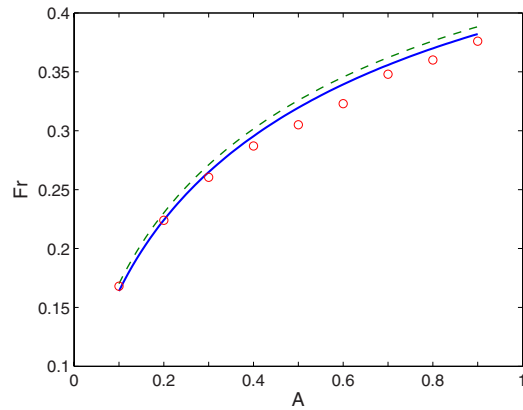


FIG. 2. (Color online) Bubble Froude number of RT instability vs Atwood number for  $Re=1000$ ,  $Bo=\infty$ , and  $\nu_l/\nu_h=1$ . The solid curve corresponds to solution (20), the dashed curve to solution (20) for  $Re=\infty$ ,  $Bo=\infty$ , and the circles to the numerical results in Ref. [12].

$$U_{RT}^{ax} \rightarrow -k\nu_h + \sqrt{\frac{2A}{1+A}g - \frac{3k}{16}\frac{\sigma}{\rho_h} + k^2\nu_h^2}. \quad (20)$$

Equation (20) shows that from the stability condition, the asymptotic velocity of an axisymmetric bubble can be reduced within 10% by surface tension in the inviscid limit.

To validate the present model, we compare with numerical results in Ref. [12]. The numerical simulations in Ref. [12] were conducted in a three-dimensional (3D) box geometry. Because a bubble in the 3D box develops to a nearly axisymmetric structure and the model assumes a local approximation near a bubble tip, the solution of the present model would be comparable to the result of the 3D box geometry. Figure 2 is the bubble Froude numbers of 3D RT instability versus the Atwood numbers for the case of  $Re=1000$ ,  $Bo=\infty$ , and  $\nu_l/\nu_h=1$ . The solid curve corresponds to solution (20) and the circles to the numerical results in Ref. [12]. The dashed curve is solution (20) for  $Re=\infty$  and  $Bo=\infty$  and is given for comparison. Figure 2 shows that the agreements between the model and the numerical results are good overall but are better for small and large density ratios.

We compare the model with numerical results for the system with surface tension. However, numerical results for RT instability with surface tension are very few, especially for a single-mode case. In fact, numerical simulations for unstable interfaces with surface tension are much more difficult than that without surface tension. We here perform numerical simulations, employing the point vortex method [13]. The vortex method follows marker particles on the interface, computing regularized integral equations for the interface. To overcome a stiffness of surface tension, the numerical algorithm is modified to an implicit time integration, while in Ref. [13], an explicit-Euler time integration is used.

In Fig. 3, the bubble velocity of RT instability in 2D from the model is compared with the numerical result of the vortex method, for the case of  $Bo=20\pi^2$ ,  $Re=\infty$ , and  $A=1$ . The initial amplitude of the sinusoidal interface is  $\eta_0 k=0.2$ . The number of marker particles used in the vortex simulation is 150. In the case of infinite density ratio, the vortex method does not need a regularizing parameter  $\delta$ , which acts as an

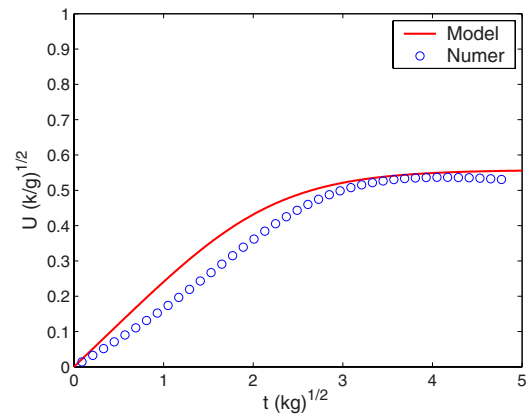


FIG. 3. (Color online) Bubble velocity of RT instability for  $Bo=20\pi^2$ ,  $Re=\infty$ , and  $A=1$ .

artificial viscosity, and only surface tension effects can be observed. Figure 3 shows a good agreement of the model and the numerical result at a late time. The agreement of the model and the numerical result at an early time is not as good as that at a late time. Note that the asymptotic bubble velocity for  $Bo=\infty$ ,  $Re=\infty$ , and  $A=1$  is 0.58.

We now apply the model to RM instability. For RM instability, we assume that surface tension is small. A surface tension dominated case is discussed below. For either case, the solution of a RM bubble can be derived from Eqs. (7) and (8) with  $g=0$ . We found that the asymptotic velocity of a RM bubble depends on a parameter  $q$  denoted as

$$q = 4k^2\nu_h^2 - \frac{\sigma}{\rho_h}k. \quad (21)$$

For  $q>0$  (viscosity dominant):

$$U_{RM}^{2D} \rightarrow -\frac{2}{3}k\nu_h + \frac{\sqrt{q}}{3} \coth\left(\frac{1+A}{3+A}k\sqrt{qt}\right). \quad (22)$$

For  $q\rightarrow 0$ :

$$U_{RM}^{2D} \rightarrow -\frac{2}{3}k\nu_h + \frac{3+A}{3(1+A)}\frac{1}{kt}. \quad (23)$$

Solutions (22) and (23) are obtained from the steady-state condition  $\eta_2 \rightarrow -k/6$ . In RM instability, this steady-state assumption for  $\eta_2$  is valid as long as  $\eta_0 k$  is large, because the exponential term in Eq. (12) is negligible. Figure 4 shows that the steady-state assumption for  $\eta_2$  is reasonable for small surface tension cases.

For  $q>0$ , Eq. (22) converges to

$$U \rightarrow \frac{1}{3}(-2k\nu_h + \sqrt{q}) + \frac{\sqrt{q}}{3}e^{-\gamma t}, \quad \gamma = \frac{2(1+A)}{3+A}k\sqrt{q}. \quad (24)$$

The limit of this solution is negative when  $\sigma>0$ , and is zero when  $\sigma=0$ . We find from Eq. (24) that in the viscosity dominant case, the velocity of a RM bubble decays much faster than the inviscid case, which decays as  $1/t$ . Note also that, in the case of  $q\rightarrow 0$ , the convergence rate is the same as the inviscid case.

The bubble velocities [Eqs. (22) and (23)] can be expressed in nondimensional forms, defining the Weber number  $We=\rho_h U_0^2 D/\sigma$  and the Reynolds number  $Re=U_0 D/\nu_h$ , where  $U_0$  is the initial velocity of the interface. Then Eq. (22) is written as

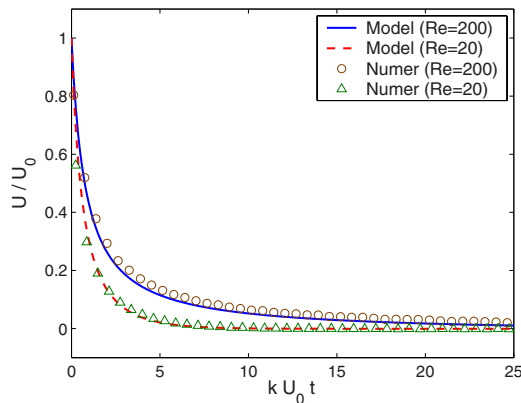


FIG. 4. (Color online) Bubble velocity of RM instability for two cases of  $Re=200$  and  $Re=20$ . The Weber number is set to  $We=2000$ , and the Atwood number is  $A=0.5$ .

$$\tilde{U} \rightarrow -\frac{4\pi}{3} \frac{1}{Re} + \frac{\sqrt{\tilde{q}}}{3} \coth\left(\frac{1+A}{3+A} \sqrt{\tilde{q}} \tilde{t}\right), \quad \tilde{q} = 4\left(\frac{2\pi}{Re}\right)^2 - \frac{2\pi}{We}, \quad (25)$$

where  $\tilde{U}=U/U_0$  is the dimensionless velocity and  $\tilde{t}=kU_0t$  the dimensionless time. Equation (23) is nondimensionalized in a similar way.

The solution of an axisymmetric RM bubble in the cylindrical geometry can be found similarly as in 2D.

$$\text{For } q > 0, \quad U_{RM}^{ax} \rightarrow -k\nu_h + \sqrt{q} \coth\left(\frac{1+A}{2} k\sqrt{q}t\right). \quad (26)$$

$$\text{For } q \rightarrow 0, \quad U_{RM}^{ax} \rightarrow -k\nu_h + \frac{2}{1+A} \frac{1}{kt}. \quad (27)$$

In the cylindrical case, the parameter  $q$  is defined by

$$q = k^2 \nu_h^2 - \frac{3k}{16} \frac{\sigma}{\rho_h}. \quad (28)$$

Figure 4 is the comparison of the results for the bubble velocity of RM instability in 2D from the present model and full numerical simulations for two cases of  $Re=200$  and  $Re=20$ . The Weber number is set to  $We=2000$ , and the Atwood number is  $A=0.5$ . The initial amplitude is  $\eta_0 k = 0.1\pi$ . The values of  $\tilde{q}$  are 0.00081 and 0.39 for the cases of  $Re=200$  and  $Re=20$ , respectively. The numerical results are obtained by employing a diffuse interface method based on a phase-field model for two-phase incompressible fluids [14]. The computational domain is  $[0, 2\pi] \times [0, 8\pi]$ , and the sinusoidal interface is initially located in the middle of the do-

main. The number of grids is  $100 \times 400$ . The details of numerical simulations will be reported elsewhere. In Fig. 4, the predictions of the model are in excellent agreements with the numerical results for both cases. Figure 4 shows that for large viscosity, the velocity of a RM bubble indeed decays fast and goes to a negative limit.

For the surface tension dominated case (or  $q < 0$ ) in RM instability, Eq. (8) gives the bubble velocity

$$U_{RM}^{2D} \sim -\frac{2}{3}k\nu_h + \frac{\sqrt{-q}}{3} \cot\left(\frac{1+A}{3+A} k\sqrt{-q}t\right) \quad (29)$$

when  $\eta_2 \sim -k/6$ . This solution shows that the bubble recedes at a late time. Equation (29) is valid, in strict sense, around the time when the bubble amplitude reaches a maximum because in this case  $\eta_2$  does not saturate to the constant limit and varies as the bubble moves back. An oscillatory mechanism that is not captured by the present model becomes influential in the time regime prior to the blow-up of Eq. (29). Therefore, solution (29) would not be valid in the vicinity of the time when it blows up, and does not imply that the bubble velocity goes to infinity in a finite time.

If surface tension is dominated in RM instability, the fluid motion near the interface at a late time should be oscillatory, representing a capillary wave [15]. The interface would bounce back and forth, and spikes may break up from the interface. The reason for the oscillatory behavior is that the interface has no external acceleration at  $t > 0$  in RM instability, and surface tension provides a restoring force to the interface. It seems that higher-order equations for the present model are needed to describe the capillary phenomena in RM instability, and this would be a next step of the research.

In conclusion, we presented a model for unstable interfaces with surface tension and viscosity and found the linear and nonlinear solutions for growth rates of single-mode RT and RM instabilities. In RT instability, both surface tension and viscosity slow the bubble velocity. The asymptotic bubble velocity is reduced greatly by a large viscosity. For RM instability, the analysis suggests a dependence of the decaying rate of the bubble velocity on the relative importance of viscosity and surface tension, and further works would be needed for modeling of the surface tension dominated case.

This work was supported by National Research Foundation of Korea Grant funded by the Korean Government under Grant No. 2009-0071664.

[1] L. Rayleigh, *Scientific Papers* (Cambridge University Press, Cambridge, England, 1900), Vol. II, p. 200.  
 [2] R. D. Richtmyer, *Commun. Pure Appl. Math.* **13**, 297 (1960).  
 [3] D. Sharp, *Physica D* **12**, 3 (1984).  
 [4] R. Bellman and R. H. Pennington, *Q. Appl. Math.* **12**, 151 (1954).  
 [5] H. W. Emmons, C. T. Chang, and B. C. Watson, *J. Fluid Mech.* **7**, 177 (1960).  
 [6] D. Layzer, *Astrophys. J.* **122**, 1 (1955).  
 [7] V. N. Goncharov, *Phys. Rev. Lett.* **88**, 134502 (2002).  
 [8] S.-I. Sohn, *Phys. Rev. E* **67**, 026301 (2003).

[9] K. O. Mikaelian, *Phys. Rev. E* **67**, 026319 (2003).  
 [10] S. I. Abarzhi, J. Glimm, and A.-D. Lin, *Phys. Fluids* **15**, 2190 (2003).  
 [11] S.-I. Sohn, *Phys. Rev. E* **75**, 066312 (2007); **78**, 017302 (2008).  
 [12] Y.-N. Young and F. E. Ham, *J. Turbul.* **7** (71), 1 (2006).  
 [13] S.-I. Sohn, *Phys. Rev. E* **69**, 036703 (2004).  
 [14] H. Ding, P. Spelt, and C. Shu, *J. Comput. Phys.* **226**, 2078 (2007).  
 [15] H. Lamb, *Hydrodynamics*, 6th ed. (Dover, New York, 1945).